

COMPARISON OF HEAT TRANSFER PHENOMENA FOR TWO DIFFERENT CRYOPRESERVATION METHODS: SLOW FREEZING AND VITRIFICATION

Anna Skorupa, Alicja Piasecka-Belkhayat

*Department of Computational Mechanics and Engineering, Silesian University of Technology
Gliwice, Poland*

anna.skorupa@polsl.pl, alicja.piasecka-belkhayat@polsl.pl

Received: 28 November 2022; Accepted: 24 February 2023

Abstract. The purpose of the research is to prepare a mathematical and numerical model for the phenomenon of heat transfer during cryopreservation. In the paper, two popular methods, slow freezing and vitrification, are compared. Furthermore, the basic model of thermal processes is supplemented by the phenomenon of phase transitions. To determine the temperature distribution during cryopreservation processes, one uses the heat transfer equation proposed by Pennes. An integral part of the energy equation is the substitute thermal capacity (STC) performed according to the concept named one domain method (fixed domain method), The numerical model is developed using the finite difference method (FDM) connected with directed interval arithmetic. The final part of the article contains the results of numerical simulations.

MSC 2010: 80A22, 65M99

Keywords: cryopreservation, slow freezing, vitrification, phase changes, finite difference method, directed interval arithmetic

1. Introduction

Cryopreservation is defined as the technique of freezing and then storing biological materials at low temperature. Cryopreservation uses cryoprotectants (CPA), which are chemical compounds designed to protect biological tissue from damage during freezing. The most commonly used cryoprotectants are glycerol (GLY), propylene glycol (PG) and dimethylsulfoxide (DMSO). Tissues must be preserved with an appropriately concentrated cryoprotectant solution in order for the cells to survive after freezing and thawing at liquid nitrogen temperature. The use of the right cryoprotectant in the right concentration guarantees a proper freezing process and adequate cell viability after thawing. During cryopreservation, CPA molecules diffuse into the intracellular space, which can disrupt the osmotic balance of the cells and be toxic to them. It is therefore essential to regulate the concentration of

CPA in the working fluid. It is important that the cryopreservation process is not toxic to cells (cytotoxicity), that is, it does not lead to cell damage or death [1, 2].

The two most common methods of cryopreservation are slow freezing and vitrification. Historically, the first attempts of cryopreservation were performed by slow freezing. It is characterized by a relatively low cooling rate and low concentrated solutions of CPA. As a result, this method is considered to have low cytotoxicity for biological cells. On the other hand, the risk of cell injury due to ice crystal formation is high [3].

A different approach is presented by vitrification. It relies on supercooling the medium with a very high cooling rate and with highly concentrated solutions of CPA. It causes the solutions to vitrify (solidify) without formation of ice crystals. Vitrification has the potential to induce cytotoxic cell damage [3].

Thermal processes are one of the phenomena to be considered during modelling cryopreservation. The basic equation that describes heat transfer is the Fourier equation [4]. It is a partial differential equation (PDE) that describes the temperature distribution induced by the transmission of a thermal wave with speed, which is infinite [5-7].

The analysis of heat transfer in soft tissues can also be performed using another parabolic equation, such as the Pennes equation [8]. This equation includes components that explain the metabolism of biological structures and the presence of blood vessels (perfusion) [5].

Examples of the modelling of phase transitions can be found in the literature [5, 9-14]. As can be seen, most of them present models related to cryosurgery. In contrast, in our work, phase changes are implemented into the energy equation to characterize the cryopreservation process.

Moreover, the literature mainly depicts deterministic models. They represent a simplification of the randomness present in living structures. On the other hand, the calculations performed for a stochastic model are time-consuming. Our proposed concept is the application of directed interval arithmetic. This approach gives results in the form of number ranges, which contain the correct results [7, 15, 16].

In our paper, the mathematical and numerical model describes the changes in the temperature distribution in a cryopreserved biological tissue. The calculation considers the phenomenon of phase transitions introduced by the one-domain method. Let us note that phase changes are an integral part of the heat transfer equation. The study investigated the cryopreservation of a sample by two different techniques: slow freezing and vitrification.

2. Materials and methods

The task demonstrates a model of a cylindrical piece of biological material immersed in a bath solution in such a way that the bath solution 'touches' the bases of the cylinder. Our model replicates the device proposed by Wang et al. [17]. The concept of the apparatus for the cryopreservation is as follows. The sample

immersed in the bath solution is placed in a test tube, which is contained in a sealed chamber. The temperature inside the chamber is regulated according to the temperature of working fluid. The temperature of the working fluid varies during the process with the cooling rate determined individually for slow freezing and for vitrification. The working fluid is liquid nitrogen, and the minimum temperature reached by them is equal to -196°C .

Let us introduce a few words about the bath solution. It is a mixture called CPTes2, consisting mainly of water and CPA, more specifically DMSO. The CPTes2 solution also contains small traces of KCl [18, 19]. The CPTes2 composition was invented by Taylor and Hunt [20] and developed by Pegg et al. [21]. The effect of the CPA included in bath solution on the behaviour of the biological material is ignored in further consideration, focusing instead on the problem of heat transfer.

It should be noted that the presented research is theoretical, as it represents a simulation performed by applying the finite difference method with implemented directed interval arithmetic rules. Figure 1 shows a schematic illustration of the modelled sample with marked considered domain.

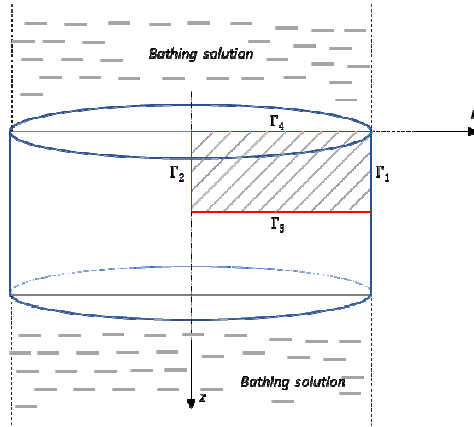


Fig. 1. Modelled sample with considered domain

2.1. Mathematical formulas

The presented model considers thermal processes in biological tissues, therefore the basis of the mathematical description is the Pennes equation [8]:

$$c_p \rho \dot{T} = \nabla \cdot (\lambda \nabla T) + w c_b (T_b - T) + Q_{met}, \quad (1)$$

where c_p is the specific heat capacity, ρ is the density, λ is the thermal conductivity, T is the temperature and $\dot{T} = \partial T / \partial t$ describes the change in the distribution of temperatures over time, w is the blood perfusion rate, c_b , T_b represent the following parameters of the blood: the specific heat capacity and the temperature, while Q with subscript *met* denotes the internal heat sources connected with metabolism.

Cryopreservation also involves phase changes phenomena that need to be introduced into the heat transfer equation (equation (1)) by an additional source function Q_{cr} [11]:

$$\left[c_p \rho - Q_{cr} \right] \dot{T} = \nabla \cdot (\lambda \nabla T) + w c_b (T_b - T) + Q_{met}, \quad (2)$$

where

$$Q_{cr} = L \dot{f}_s, \quad (3)$$

while L is the latent heat and $\dot{f}_s = \partial f_s / \partial t$ represents the local change in volume of the frozen state in the intermediate region.

It is worth mentioning that during cryopreservation, three subdomains can be distinguished in the sample, depending on the physical state that it is presented in the given point. These are the following regions: natural, intermediate, and below freezing (melting) point. The function f_s takes on a different value depending on the physical state considered in the subdomain. For the natural state and the state below the freezing (melting) point, this function is equal to 0 and 1. Whereas, in the intermediate region, the assumption is established that $f_s = f_s(T)$, hence:

$$Q_{cr} = L \frac{\partial f_s}{\partial t} = L \frac{df_s}{dT} \dot{T}. \quad (4)$$

Let us introduce the above relationship (equation (4)) into the heat transfer equation (equation (2)):

$$\left[c_p \rho - L \frac{df_s}{dT} \right] \dot{T} = \nabla \cdot (\lambda \nabla T) + w c_b (T_b - T) + Q_{met}, \quad (5)$$

and define the substitute thermal capacity C_{STC} as:

$$C_{STC} = \left[c_p \rho - L \frac{df_s}{dT} \right]. \quad (6)$$

Knowing the general form of the heat transfer equation including phase transformations, it is useful to develop the above formula using directed interval arithmetic. The thermal conductivity (λ) and the volumetric specific heat ($c_v = c_p \cdot \rho$) are introduced into the mathematical model as interval numbers. As a consequence, the results obtained are also in the form of intervals. The presence of interval numbers is implied in the equations by dashes over the variables. More information about rules of the directed interval arithmetic can be found in [15].

The sample is considered in a cylindrical system, hence the heat transfer equation is as follows:

$$\begin{aligned} \bar{C}_{STC}(\bar{T}) \frac{\partial \bar{T}(r, z, t)}{\partial t} = & \frac{1}{r} \frac{\partial}{\partial r} \left(r \bar{\lambda}(\bar{T}) \frac{\partial \bar{T}(r, z, t)}{\partial r} \right) + \frac{\partial}{\partial z} \left(\bar{\lambda}(\bar{T}) \frac{\partial \bar{T}(r, z, t)}{\partial z} \right) + \\ & + \bar{Q}_{met}(\bar{T}) + \bar{w}(\bar{T}) c_b [T_b - \bar{T}(r, z, t)] \end{aligned} \quad (7)$$

where r, z are the geometric coordinates of the cylindrical coordinate system and t is the time. Please note that the thermophysical parameters and the internal heat source depend on the temperature. These variables are determined in different ways based on the physical state of the given subdomain. For the natural state and below the freezing (melting) point, constant values are assumed; whereas for the intermediate region, a linear function is established. They are defined from the relationships [5]:

$$\bar{C}_{STC}(\bar{T}) = \begin{cases} \bar{c}_N & \bar{T} > T_l, \\ \bar{c}_{in} + \frac{L}{T_l - T_s} & T_s \leq \bar{T} \leq T_l, \\ \bar{c}_f & \bar{T} > T_s, \end{cases} \quad (8)$$

$$\bar{\lambda}(\bar{T}) = \begin{cases} \bar{\lambda}_N & \bar{T} > T_l, \\ \bar{\lambda}_{in} & T_s \leq \bar{T} \leq T_l, \\ \bar{\lambda}_f & \bar{T} > T_s, \end{cases} \quad (9)$$

$$\bar{w}(\bar{T}) = \begin{cases} w_N & \bar{T} > T_l, \\ \frac{w_N}{T_l - T_s} [\bar{T}(r, z, t) - T_s] & T_s \leq \bar{T} \leq T_l, \\ 0 & \bar{T} > T_s, \end{cases} \quad (10)$$

$$\bar{Q}_{met}(\bar{T}) = \begin{cases} Q_{metN} & \bar{T} > T_l, \\ \frac{Q_{metN}}{T_l - T_s} [\bar{T}(r, z, t) - T_s] & T_s \leq \bar{T} \leq T_l, \\ 0 & \bar{T} > T_s, \end{cases} \quad (11)$$

where T with the subscripts l and s represent the start and the end of the phase changes processes, as well as the subscripts N, in, f denote states: natural, intermediate, and below freezing (melting) point, respectively.

The heat transfer equation is supplemented with an initial condition $\bar{T} = T_0$. The boundary conditions are also determined. At the boundary, where the thermal transfer occurs between the sample and the working fluid ($\Gamma = \Gamma_4: z = 0$), the Robin

condition is proposed: $-\mathbf{n}\bar{\lambda}\nabla\bar{T} = \alpha[\bar{T}(r, z, t) - T_{bath}]$; where \mathbf{n} is the normal vector, α is natural convection heat transfer coefficient and T_{bath} is the temperature of the bath solution. At the other boundaries ($\Gamma = \Gamma_1: r = R; \Gamma = \Gamma_2: r = 0, \Gamma = \Gamma_3: z = H$), the adiabatic condition is applied: $\bar{q} = -\mathbf{n}\bar{\lambda}\nabla\bar{T} = 0$; where \bar{q} is the interval heat flux.

2.2. Numerical model

The finite difference method (FDM) was used to solve the heat transfer equation. At the beginning, simulation time and sample domain should be discretized. A fixed time grid with a step $\Delta t = t^{f+1} - t^f$ was established as follows:

$$t^0 < t^1 < \dots < t^{f-2} < t^{f-1} < t^f < \dots < t^F < \infty. \quad (12)$$

On the other hand, a regular geometric grid was applied to the sample domain according to the concept of five-points star (Fig. 2). As can be seen, the boundary nodes do not coincide with the boundary line of the sample, but are $0.5h$ and $0.5k$ away from it (h and k mesh grid in the r - and z -direction). This ensures better approximation of boundary conditions of the 2nd and 3rd type [15].

For internal nodes (points (i, j) , where $i = 2, 3, \dots, n-1$ and $j = 2, 3, \dots, m-1$; n and m are the number of nodes), the temperature distribution is determined according to the concept presented in [15].

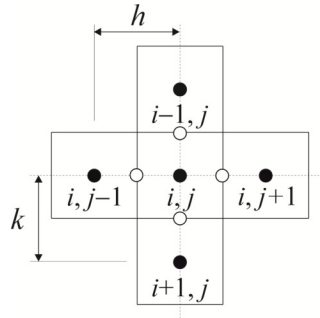


Fig. 2. Five-points star

By substituting the corresponding differential quotients into the energy equation, the temperature at the given internal node (i, j) has the following form:

$$\begin{aligned} \bar{T}_{i,j}^f = \bar{T}_{i,j}^{f-1} + \frac{\Delta t}{(\bar{C}_{STC})_{i,j}^{f-1}} & \left[\left(\sum_{a=1}^4 \frac{\Phi_e}{\bar{R}_e^{f-1}} (\bar{T}_e^{f-1} - \bar{T}_{i,j}^{f-1}) \right) + \right. \\ & \left. + \bar{Q}_{met}(\bar{T}_{i,j}^{f-1}) + \bar{w}(\bar{T}_{i,j}^{f-1}) c_b (T_b - \bar{T}_{i,j}^{f-1}) \right], \end{aligned} \quad (13)$$

where: $i = 2, 3, \dots, n-1$ and $j = 2, 3, \dots, m-1$ and individual a corresponds to $e = \{(i, j+1); (i, j-1); (i+1, j); (i-1, j)\}$.

In the above equation, the shape function Φ and the interval thermal resistance \bar{R} are introduced and is defined as:

$$\left\{ \begin{array}{l} \Phi_e = \frac{1}{h} \left(1 - \frac{h}{2r_{i,j}} \right) \quad \text{if } e = (i, j-1), \\ \Phi_e = \frac{1}{h} \left(1 + \frac{h}{2r_{i,j}} \right) \quad \text{if } e = (i, j+1), \\ \Phi_e = \frac{1}{k} \quad \text{if } e = \{(i+1, j) \text{ or } (i-1, j)\}, \end{array} \right. \quad (14)$$

where $r_{i,j}$ is the radial coordinate of the node (i, j) .

Meanwhile, the interval thermal resistances are of the form:

$$\begin{aligned} \bar{R}_e^{f-1} &= \frac{h}{2\bar{\lambda}(\bar{T}_{i,j}^{f-1})} + \frac{h}{2\bar{\lambda}(\bar{T}_e^{f-1})} \quad \text{if } e = \{(i, j+1) \text{ or } (i, j-1)\}, \\ \bar{R}_e^{f-1} &= \frac{k}{2\bar{\lambda}(\bar{T}_{i,j}^{f-1})} + \frac{k}{2\bar{\lambda}(\bar{T}_e^{f-1})} \quad \text{if } e = \{(i+1, j) \text{ or } (i-1, j)\}. \end{aligned} \quad (15)$$

Similar derivations can be made for boundary nodes. For example, for $\Gamma = \Gamma_4$; $z = 0$, the temperature at the node is defined as:

$$\begin{aligned} \bar{T}_{1,j}^f &= \bar{T}_{1,j}^{f-1} + \frac{\Delta t}{(\bar{C}_{STC})_{1,j}^{f-1}} \left[\left(\sum_{a=1}^3 \frac{\Phi_e}{\bar{R}_e^{f-1}} (\bar{T}_e^{f-1} - \bar{T}_{1,j}^{f-1}) + \frac{\Phi_{i-1,j}}{\bar{R}_\alpha^{f-1}} (\bar{T}_{bath}^{f-1} - \bar{T}_{1,j}^{f-1}) \right) + \right. \\ &\quad \left. + \bar{Q}_{met}(\bar{T}_{1,j}^{f-1}) + \bar{w}(\bar{T}_{1,j}^{f-1}) c_b (T_b - \bar{T}_{1,j}^{f-1}) \right], \end{aligned} \quad (16)$$

where $j = 2, 3, \dots, m-1$, individual a corresponds to $e = \{(i, j+1); (i, j-1); (i+1, j)\}$ and

$$\bar{R}_\alpha^{f-1} = \frac{k}{2\bar{\lambda}(\bar{T}_{1,j}^{f-1})} + \frac{1}{\alpha}. \quad (17)$$

However, for $\Gamma = \Gamma_3$; $z = H$, the temperature can be calculated as:

$$\begin{aligned} \bar{T}_{n,j}^f &= \bar{T}_{n,j}^{f-1} + \frac{\Delta t}{(\bar{C}_{STC})_{n,j}^{f-1}} \left[\left(\sum_{a=1}^3 \frac{\Phi_e}{\bar{R}_e^{f-1}} (\bar{T}_e^{f-1} - \bar{T}_{n,j}^{f-1}) + \bar{q} \cdot \Phi_{i+1,j} \right) + \right. \\ &\quad \left. + \bar{Q}_{met}(\bar{T}_{n,j}^{f-1}) + \bar{w}(\bar{T}_{n,j}^{f-1}) c_b (T_b - \bar{T}_{n,j}^{f-1}) \right], \end{aligned} \quad (18)$$

where $j = 2, 3, \dots, m - 1$ and individual a corresponds to $e = \{(i, j + 1); (i, j - 1); (i - 1, j)\}$. The temperatures in the other boundary nodes are determined analogically.

3. Results

Example calculations have been performed for a biological tissue considered in a cylindrical coordinate system. A two-dimensional (2D) axisymmetric region was analysed with the dimensions $H = 0.02$ m and $R = 0.02$ m.

The tissue model includes blood vessels; therefore, blood parameters should be mentioned, such as the blood temperature $T_b = 37^\circ\text{C}$, the specific heat capacity of the blood $c_b = 3770 \text{ J}\cdot\text{kg}^{-1}\cdot\text{K}^{-1}$ and the perfusion in the natural state $w_N = 0.53 \text{ kg}\cdot\text{m}^{-3}\cdot\text{s}^{-1}$. In the natural state, the sample is also characterized by an internal heat source related to metabolism $Q_{met N} = 250 \text{ W}\cdot\text{m}^{-3}$. The limiting temperatures between the particular states are assumed to be $T_l = -1^\circ\text{C}$ and $T_s = -8^\circ\text{C}$. Depending on these temperatures, the specific values of the interval thermophysical parameters are selected: $\bar{\lambda}_N = [0.494; 0.546] \text{ W}\cdot\text{m}^{-1}\cdot\text{K}^{-1}$ and $\bar{c}_N = [3.42 \cdot 10^6; 3.78 \cdot 10^6] \text{ J}\cdot\text{K}^{-1}\cdot\text{m}^{-3}$ for a natural state, $\bar{\lambda}_{in} = [1.197; 1.323] \text{ W}\cdot\text{m}^{-1}\cdot\text{K}^{-1}$ and $\bar{c}_{in} = [47.412; 52.403] \text{ J}\cdot\text{K}^{-1}\cdot\text{m}^{-3}$ for an intermediate region, $\bar{\lambda}_f = [1.9; 2.1] \text{ W}\cdot\text{m}^{-1}\cdot\text{K}^{-1}$ and $\bar{c}_f = [1.834; 2.027] \text{ J}\cdot\text{K}^{-1}\cdot\text{m}^{-3}$ for a state below freezing (melting) point. However, the latent heat for this system that is relevant in the intermediate region is equal to $L = 3.3 \cdot 10^8 \text{ J}\cdot\text{m}^{-3}$ [5].

Let us introduce the parameters related to the initial and boundary conditions: the initial temperature is established as $T_0 = 37^\circ\text{C}$, the natural convection heat transfer coefficient is equal to $\alpha = 525 \text{ W}\cdot\text{m}^{-2}\cdot\text{K}^{-1}$ [18]. It is also worth mentioning two methods of controlling the temperature of the bath solution. During the simulation of slow freezing, the temperature decreased (increased) at a cooling rate equal to $\pm 1 \text{ K}\cdot\text{min}^{-1}$, in accordance with studies performed by Mazur [22]. On the other hand, cryopreservation by vitrification is also analysed, and the cooling rate is $\pm 100 \text{ K}\cdot\text{min}^{-1}$ [3]. The cooling process is stopped, and the heating process begins when the temperature of bath solution is equal to $T_{bath} = -196^\circ\text{C}$, which corresponds to the temperature of the working fluid (liquid nitrogen).

The calculations have been carried out by the finite difference method (FDM) applying the rules of directed interval arithmetic described, e.g. in [15]. The mesh steps are $h = k = 0.0002$ m ($m = n = 100$) and the time step is $\Delta t = 0.005$ s.

In our research, two cases of cryopreservation have been investigated: slow freezing and vitrification. Figure 3 depicts the changes in the mean value of the interval temperature for the six selected points and the temperature of the bath solution (solid line) over time. The following point is considered: A(0.0001 m; 0.0001 m), B(0.0009 m; 0.0001 m), C(0.0019 m; 0.0001 m), D(0.0029 m; 0.0001 m), E(0.0039 m; 0.0001 m), F(0.0049 m; 0.0001 m). Please note that for slow freezing, only the cooling process was computed due to the very long time of the simulation.

On the other hand, vitrification is much faster, therefore calculations were performed for cooling and heating.

Comparing these graphs, significant differences in the mean values of the interval temperature between different points occur, e.g. when the temperature of the bathing solution reaches its minimum value.

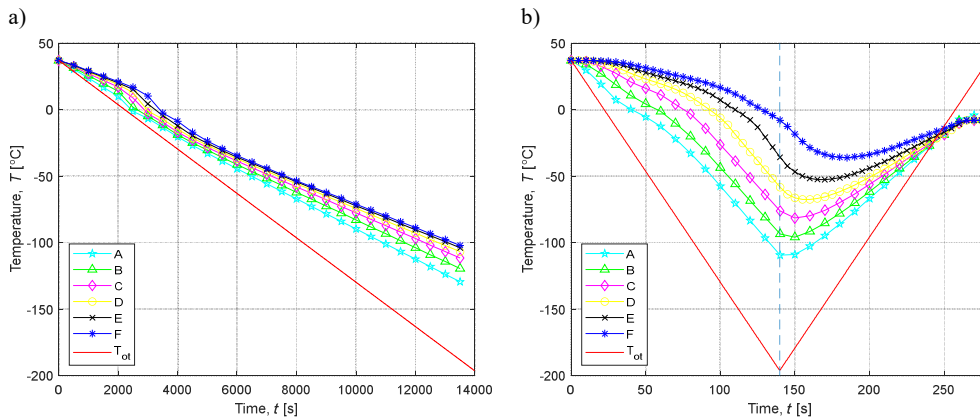


Fig. 3. History of mean value of interval temperature over time for: a) slow freezing, b) vitrification

As mentioned before, interval numbers have been introduced into the model, and the temperatures obtained are also intervals. Figure 4 presents the distribution of the interval temperature at the first 20 s of the simulation for the point B. In addition, Table 2 provides examples of interval temperatures for the point B in given time. It can be concluded that as the temperature decreases, the width of the intervals increases significantly, as well.

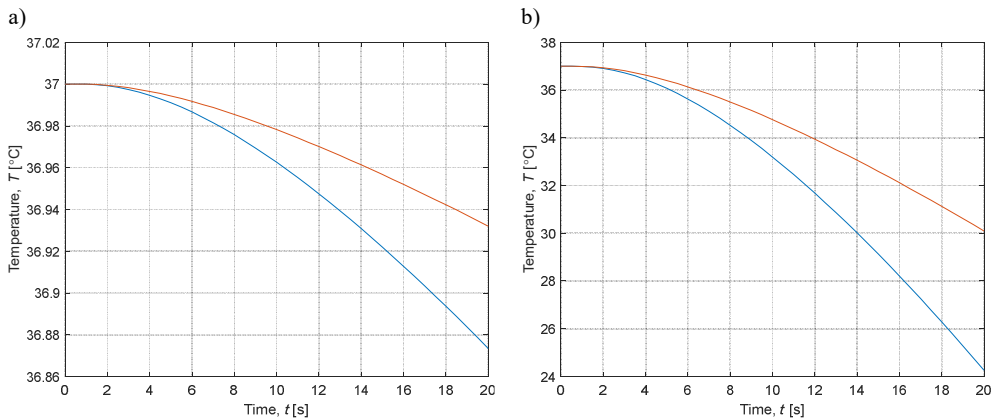


Fig. 4. History of interval temperature for point B for: a) slow freezing, b) vitrification

Table 2. Interval temperature in given moment of simulation for the point B

Time t [s]	Interval temperature \bar{T} [°C]	
	Slow freezing	Vitrification
0	[37.00; 37.00]	[37.00; 37.00]
10	[36.96; 36.97]	[33.20; 34.77]
20	[36.87; 36.93]	[24.26; 29.84]
30	[36.76; 36.88]	[12.95; 24.53]
40	[36.63; 36.82]	[3.80; 17.70]
50	[36.50; 36.75]	[0.28; 8.35]
139.5	[-35.13; -36.14]	[-142.12; -43.45]
13980	[-195.83; -53.11]	–

In order to better illustrate the distribution of the mean values of the interval temperatures in the sample, Figure 5 for slow freezing and Figure 6 for vitrification have been prepared. Two distribution maps have been made for each cryopreservation method: in the middle of the freezing processes and when $T_{bath} = -196^\circ\text{C}$.

For slow freezing, in the middle of time simulation, the wide intermediate region exists. When the temperature of the bath solution is at its minimum, the entire area is below its freezing (melting) point. During vitrification, the intermediate region is much smaller than it is for slow freezing. It is also worth noting that in the moment when the temperature of bath solution reach the assumed minimum temperature, all three physical states occur in the domain under consideration.

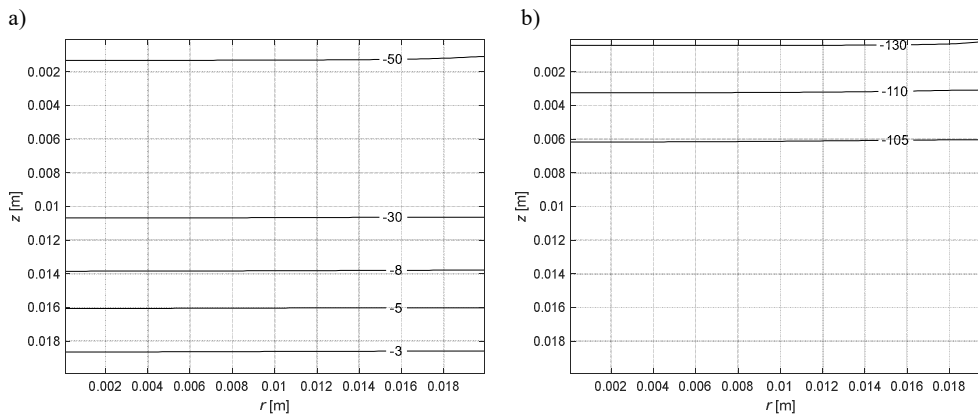


Fig. 5. Distribution of mean value of interval temperature for slow freezing method:

a) $t = 6990$ s, $T_{bath} = -79.5^\circ\text{C}$, b) $t = 13980$ s, $T_{bath} = -196^\circ\text{C}$

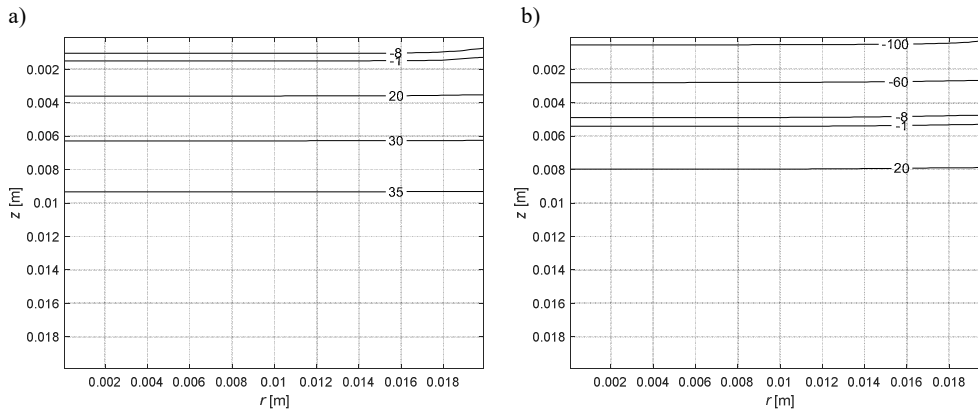


Fig. 6. Distribution of mean value of interval temperature for the vitrification method:
 a) $t = 70$ s, $T_{bath} = -79.67^\circ\text{C}$, b) $t = 139.8$ s, $T_{bath} = -196^\circ\text{C}$

4. Discussion and conclusions

The paper presents a mathematical and numerical model of the cryopreservation process performed by two commonly used methods: slow freezing and vitrification. In particular, the analysis describes the heat transfer in a 2D sample considered in a cylindrical system. In addition, interval numbers were included in the model to introduce the nondeterministic character of the thermophysical parameters. As a result, calculations were conducted on the basis of directed interval arithmetic rules implemented into the FDM.

When comparing the two methods in the context of the obtained results, the difference in simulation times certainly should be pointed out. It can be concluded that the temperature distribution for slow freezing is more regular and stabilized as a result of the time of the process. When the temperature of the bath reaches a defined minimum, the temperature in the entire area is below the freezing (melting) point. It can be assumed that it is timing that facilitates heat transport. In addition, as noted by Mazur [22], slow freezing with an adequate cooling rate allows osmotic transport of water from the intracellular space to the extracellular matrix.

In contrast, by analysing the temperature distribution in the middle of the freezing simulation, a considerable area covered by the intermediate region can be observed. This indicates a high risk of ice crystal formation. It is important to note that to assess the degree of potential sample damage, it is necessary to investigate mass transport phenomena and the degree of crystallization, as shown, e.g. in [7, 18, 23, 24].

The results are different for the vitrification method. When the temperature of the bath solution is equal to the minimum temperature of the working fluid, all three physical states are presented in the sample, which could suggest incomplete freezing of the sample. A similar situation occurs in the middle of a freezing simulation. However, it must be remembered that the main idea of this method is to

obtain amorphous ice, where the solution solidifies (vitrifies) without forming ice crystals. Vitrification is conducted using a highly concentrated CPA solution, which can cause injury to the sample as a result of cytotoxicity. The impact of CPA is described, e.g., by the osmotic transport phenomenon presented in [7, 18].

In summary, when preparing a model for the thermal transfer during cryopreservation, it is important to consider the phenomenon of phase transitions. There is a plan, in the future, to add also mass transfer and osmotic transport information to the model.

Acknowledgment

The research was partially funded from financial resources from the statutory subsidy of the Faculty of Mechanical Engineering, Silesian University of Technology, in 2022.

References

- [1] Jang, T.H., Park, S.C., Yang, J.H., Kim, J.Y., Seok, J.H., Park, U.S., Choi, C.W., Lee, S.R., & Han, J. (2017). Cryopreservation and its clinical applications. *Integrative Medicine Research*, 6(1), 12-18. DOI: 10.1016/j.imr.2016.12.001.
- [2] Jungare, K.A., Radha, R., & Sreekanth, D. (2022). Cryopreservation of biological samples – A short review. *Materials Today: Proceedings*, 51, 1637-1641. DOI: 10.1016/j.matpr.2021.11.203.
- [3] Xu, F., Moon, S., Zhang, X., Shao, L., Song, Y.S., & Demirci, U. (2010). Multi-scale heat and mass transfer modelling of cell and tissue cryopreservation. *Philosophical Transactions of the Royal Society A: Mathematical, Physical and Engineering Sciences*, 368(1912), 561-583. DOI: 10.1098/rsta.2009.0248.
- [4] Fourier, J.B.J. (1882). *Théorie analytique de la chaleur*. Firmin Didot.
- [5] Mochnacki, B., & Majchrzak, E. (2017). Numerical model of thermal interactions between cylindrical cryoprobe and biological tissue using the dual-phase lag equation. *International Journal of Heat and Mass Transfer*, 108, 1-10. DOI: 10.1016/j.ijheatmasstransfer.2016.11.103.
- [6] Popczyk, O., & Dziaekiewicz, G. (2022). Kansa method for solving initial-value problem of hyperbolic heat conduction in nonhomogeneous medium. *International Journal of Heat and Mass Transfer*, 183, 122088. DOI: 10.1016/j.ijheatmasstransfer.2021.122088.
- [7] Piasecka-Belkhat, A., & Skorupa, A. (2022). Application of interval arithmetic in numerical modeling of cryopreservation process during cryoprotectant loading to microchamber. *Numerical Heat Transfer, Part A: Applications*, 1-19. DOI: 10.1080/10407782.2022.2105078.
- [8] Pennes, H.H. (1948). Analysis of tissue and arterial blood temperatures in the resting human forearm. *Journal of Applied Physiology*, 1(2), 93-122.
- [9] Ahmadikia, H., & Moradi, A. (2012). Non-Fourier phase change heat transfer in biological tissues during solidification. *Heat and Mass Transfer*, 48(9), 1559-1568. DOI: 10.1007/s00231-012-1002-1.
- [10] Ge, M.Y., Shu, C., Yang, W.M., & Chua, K.J. (2017). Incorporating an immersed boundary method to study thermal effects of vascular systems during tissue cryo-freezing. *Journal of Thermal Biology*, 64, 92-99. DOI: 10.1016/j.jtherbio.2017.01.006.
- [11] Majchrzak, E., Mochnacki, B., Dziaekiewicz, M., & Jasiński, M. (2011). Numerical modelling of hyperthermia and hypothermia processes. *Advanced Materials Research*, 268-270, 257-262. DOI: 10.4028/www.scientific.net/AMR.268-270.257.

- [12] Singh, S., & Kumar, S. (2015). freezing of biological tissues during cryosurgery using hyperbolic heat conduction model. *Mathematical Modelling and Analysis*, 20(4), 443-456. DOI: 10.3846/13926292.2015.1064486.
- [13] Wang, Z., Zhao, G., Wang, T., Yu, Q., Su, M., & He, X. (2015). Three-dimensional numerical simulation of the effects of fractal vascular trees on tissue temperature and intracellular ice formation during combined cancer therapy of cryosurgery and hyperthermia. *Applied Thermal Engineering*, 90, 296-304. DOI: 10.1016/j.applthermaleng.2015.06.103.
- [14] Deng, Z.-S., & Liu, J. (2005). Numerical simulation of selective freezing of target biological tissues following injection of solutions with specific thermal properties. *Cryobiology*, 50(2), 183-192. DOI: 10.1016/j.cryobiol.2004.12.007.
- [15] Skorupa, A., & Piasecka-Belkhatay, A. (2020). Numerical modeling of heat and mass transfer during cryopreservation using interval analysis. *Applied Sciences*, 11(1), 302. DOI: 10.3390/app11010302.
- [16] Moore, R.E. (1966). *Interval Analysis*. Printice-Hall.
- [17] Wang, L., Pegg, D.E., Lorrison, J., Vaughan, D., & Rooney, P. (2007). Further work on the cryopreservation of articular cartilage with particular reference to the liquidus tracking (LT) method. *Cryobiology*, 55(2), 138-147. DOI: 10.1016/j.cryobiol.2007.06.005.
- [18] Yu, X., Zhang, S., & Chen, G. (2019). Modeling the addition/removal of dimethyl sulfoxide into/from articular cartilage treated with the liquidus-tracking method. *International Journal of Heat and Mass Transfer*, 141, 719-730. DOI: 10.1016/j.ijheatmasstransfer.2019.07.032.
- [19] Pegg, D.E., Wusteman, M.C., & Wang, L. (2006). Cryopreservation of articular cartilage. Part 1: Conventional cryopreservation methods. *Cryobiology*, 52(3), 335-346. DOI: 10.1016/j.cryobiol.2006.01.005.
- [20] Taylor, M.J., & Hunt, C.J. (1985). A new preservation solution for storage of corneas at low temperatures. *Current Eye Research*, 4(9), 963-973. DOI: 10.3109/02713689509000003.
- [21] Pegg, D.E., Wang, L., & Vaughan, D. (2006). Cryopreservation of articular cartilage. Part 3: The liquidus-tracking method. *Cryobiology*, 52(3), 360-368. DOI: 10.1016/j.cryobiol.2006.01.004.
- [22] Mazur, P. (1963). Studies on rapidly frozen suspensions of yeast cells by differential thermal analysis and conductometry. *Biophysical Journal*, 3(4), 323-353. DOI: 10.1016/S0006-3495(63)86824-1.
- [23] Shi, M., Feng, S., Zhang, X., Ji, C., Xu, F., & Lu, T.J. (2018). Droplet based vitrification for cell aggregates: Numerical analysis. *Journal of the Mechanical Behavior of Biomedical Materials*, 82, 383-393. DOI: 10.1016/j.jmbbm.2018.03.026.
- [24] Zhou, X., Liu, Z., Liang, X.M., Shu, Z., Du, P., & Gao, D. (2013). Theoretical investigations of a novel microfluidic cooling/warming system for cell vitrification cryopreservation. *International Journal of Heat and Mass Transfer*, 65, 381-388. DOI: 10.1016/j.ijheatmasstransfer.2013.06.022.